



## EXPERIMENTAL STUDY FOR TRANSIENT HEAT TRANSFER FROM A FLAT PLATE UNDER AIR IMPINGEMENT

Dr. Adnan A. Abdul Rasool<sup>1</sup>, Dr. Dhamyaa Saad Khudhur<sup>2</sup>, Sarah Ahmed Oudah<sup>3</sup>

- 1) Prof. Dr., Mechanical Engineering Department, Al-Mustansiriayah University, Baghdad, Iraq.
- 2) Lecturer, Mechanical Engineering Department, Al-Mustansiriayah University, Baghdad, Iraq.
- 3) M.Sc., Mechanical Engineering Department, Al-Mustansiriayah University, Baghdad, Iraq

**Abstract:** The present work represent an experimental study to verify the transient heat transfer characteristics of a target plate under air impingement from different orifice sizes ( $D=5, 10, 15$  and  $20\text{mm}$ ), with orifice to plate distance ratio ( $H/D=2, 4, 6$  and  $8$ ). Air jet velocities is varied in the range ( $U_j=18-40\text{m/s}$ ) representing ( $Re=7100-11900$ ). The heat transfer coefficient on the target plate are calculated on the basis of two dimensional infinite case. The local variation of Nusselt number in the transient period  $\tau_o$  is measured. The values are compared to that at the steady state condition. Results show that the Nusselt values are maximum at state of impingement process and decays with time on proceeding of the cooling process and also with space reaching the plate edge.

**Keywords:** *Transient impingement, jet cooling, heat transfer on a flat plate*

### دراسة عملية لانتقال الحرارة الانتقالي من صفيحة مستوية تحت تبريد الهواء التصادمي

**الخلاصة:** يتمثل العمل الحالي دراسة تجريبية للتحقق من خصائص الانتقال الحراري الانتقالي لصفيحة الهدف في ظل اصطدام الهواء من احجام اقطار مختلفة ( $D=5,10,15,20\text{mm}$ )، مع المسافة النسبية بين القطر و الصفيحة ( $H/D=2,4,6,8$ ). تتنوع سرعات الهواء الخارجة من فوهة القطر ضمن فترة ( $U_j=18-40\text{ م/ث}$ ) تمثل ( $Re=7100-11900$ ). يتم احتساب معامل انتقال الحرارة على الصفيحة الهدف على أساس حالة لانهاية الأبعاد الثنائية. يتم قياس تباين عدد نسلت الموضعي في الفترة الانتقالية  $\tau_o$ . تتم مقارنة القيم مع الحالة مستقرة. وأظهرت النتائج أن قيم نسلت هي الحد الأقصى في حالة عملية اصطدام و يضمحل مع مرور الوقت على إجراء عملية التبريد و أيضا مع المسافة إلى حافة الصفيحة.

## 1. Introduction

The impinging jet can be described as a phenomenon in which the fluid exiting from a nozzle or orifice and hits a wall or solid surface usually at normal angle[1]. Impingement cooling is widely used due to high rate of heat transfer removal with different application as that used in turbine blade impingement cooling, drying of paper and textiles and electrical equipment cooling, ...etc [2]. A lot of research works are published on impingement process and different factors affecting its efficiency including jet velocity, orifice diameter, orifice shape, orifice to plate distance ratio and

\*Corresponding Author [damiaasaad@yahoo.com](mailto:damiaasaad@yahoo.com).

number of orifices and its distribution in case of studying multi jet condition. The transient process during cooling period in impingement process takes its importance due to increasing rate of increase in heat flux and its rate in many applications specially in electric applications due to high rate of electric processing, which can increase component temperature suddenly, which needs an instantaneous increase in cooling capacity which means that the cooling process undergoes a transient period[3].

Many techniques have theoretically and experimentally studied the steady and transient heat transfer by impingement jet. Islam and Rezwan [4] focused on performance of fire protective clothing under the flame blast condition by using a hot air on base plate with/without protective fabric. The air jet temperature was (125°C) and jet velocity was (15 m/s and 19 m/s) and the nozzle diameter was (25.4mm). The longitudinal distance to nozzle diameter was used (  $H/d=2,4$  and 6), and the radial distance to the nozzle diameter was used (  $r/d= -4.5$  to 4.5). The experimental results show the heat transfer rate decreased when used the protective fabric. Mark [5] studied the effect of heating for steady state and transient heat transfer of a patterned plate under liquid jet impingement by using (H<sub>2</sub>O) as a working fluid. Results done for Reynolds number range from (500 to 1000) and indentation depths range from (0.125 to 0.5mm). The results show for steady state that increase heat transfer coefficient and Nusselt number with increasing Reynolds number, thermal conductivity for materials have large effect on temperatures of plate. The results for transient state show that the temperatures interface increased with time till reached the steady state, higher thermal conductivity and selection of material have large effect of time required till reached steady state, average heat transfer coefficient and Nusselt number decreased with time for all geometry. Colin and Tadhg [6] carried out the local heat transfer coefficient for single, axisymmetric, submerged and confined impinging jet for air and water jets. Reynolds number range from (1000 to 20000), jet diameter (0.5, 1 and 1.5mm) and jet to target distance ratio range from ( $H/d=1$  to 4). It's found that the average heat transfer increased with decreasing jet diameter due to higher jet velocities. When used air jets, it's found the secondary peaks presented at low jet to target distance ratio ( $H/d$ ) and high Reynolds number. At water jets, also found secondary peaks, these observed at low Reynolds number of 1000 and low  $H/d$  of 1. Anwarullah [7] studied the effect of nozzle to surface spacing ( $H/d$ ) on impinging jet heat transfer and fluid flow. Results are for Reynolds number range from (6000 to 23000), nozzle to surface spacing ( $H/d=2,4,8$  and 10) and nozzle diameter of ( $d=5$ mm). The results show that the effect of nozzle aspect was less when increase the nozzle to surface spacing ( $H/d$ ), and increase heat transfer rate as decreasing in jet spacing. Correlation is developed for stagnation Nusselt number in term of Reynolds number, Prandtl number, nozzle to surface spacing and nozzle aspect ratio, as follows:

$$Nu_{cor} = 0.8(Re_d)^{0.5}(Pr)^{0.36}(H/D)^{-0.06} .$$

In present study, experimental tests on cooling rate of target plate in transient state during air jet impingement of different orifice diameter sizes of (5,10,15 and 20mm) and to verify its behavior under different conditions of jet velocity range from (18-40m/s) and orifice to plate distance ratio at range (2,4,6 and 8). Local and average heat transfer coefficients are estimated on the basis of semi- infinite transient case for the flat

plate tested and Nusselt number are then calculated. The transient period for the plate is measured and found in the range of (0 – 2000sec.) for all tested cases. The steady state heat transfer coefficients values are then compared to transient state values and correlations are developed for transient and steady state conditions.

## 2. Experimental Setup

The study has been carried out by using experimental device consists of air blower, pipe, orifice, heated plate fitted at test section in which air impinges on it and flows horizontally on the plate surface at which a wall jet is developed as shown in Fig. 1 . Air blower is of 6 m<sup>3</sup>/min blowing capacity at 2800 rpm, flexible duct of 50mm diameter and 2.5m length are used to connect air duct to the air blower and used ring-type tightener to prevent air leakage, P.V.C pipe with 50mm diameter and 75cm length with a straightener inserted at pipe made of 60 circular small diameter to reduce turbulence intensity for incoming air each cell 5mm diameter and 10cm length (this air straightener is made according to British standard 1042.[16]).

Four orifice diameter as shown in Fig. 2 provided of (5,10,15 and 20mm) matching of a fully developed turbulent pipe flow for jet velocity range from (18-40m/s) with bypass valve used to control velocity range fixed near pipe inlet, (staco variable transformers, Variac) are used to supply electrical power to heater wire with constant voltage level i.e. a constant heat flux in range of (0-220 V) and (0-0.9 A). The test section of size 35×35×9.6cm height, consist of wood blocks (2.5cm) thickness in four sides to prevent heat transfer to surrounding due to low thermal conductivity as shown in Fig. 3, target plate made of stainless steel with size (30×30cm<sup>2</sup> and 0.4mm thickness) fitted at test section where air impinges on it as shown in Fig. 4.

A high thermal conductivity of Duralumin Alloy plate with (30×30cm<sup>2</sup> and 0.6mm thickness) fixed between stainless steel plate and heater to ensure uniform distribution of heat through the plate surface. Heater wire of resistance (23 Ω) fixed and wrapped below the Duralumin Alloy plate. Non-silicon heat transfer compound are then used between stainless steel plate and Duralumin Alloy plates and heater to ensure a reliable thermal coupling and heat dissipation.

A polyurethane insulation foam are then used beneath heater to fill gaps and to reduce heat losses by conduction to the outer portion of test section. 12 calibrated thermocouples type-K are fitted below the stainless steel plate to measure temperature distribution along plate centerline, then two additional thermocouples are placed to calculate heat losses beneath the heated plate, one below test section and other between heater and insulation foam as shown in Fig. 3. Adjustable base used under the test section to vary height of target plate relative to the orifice to get different H/D values.

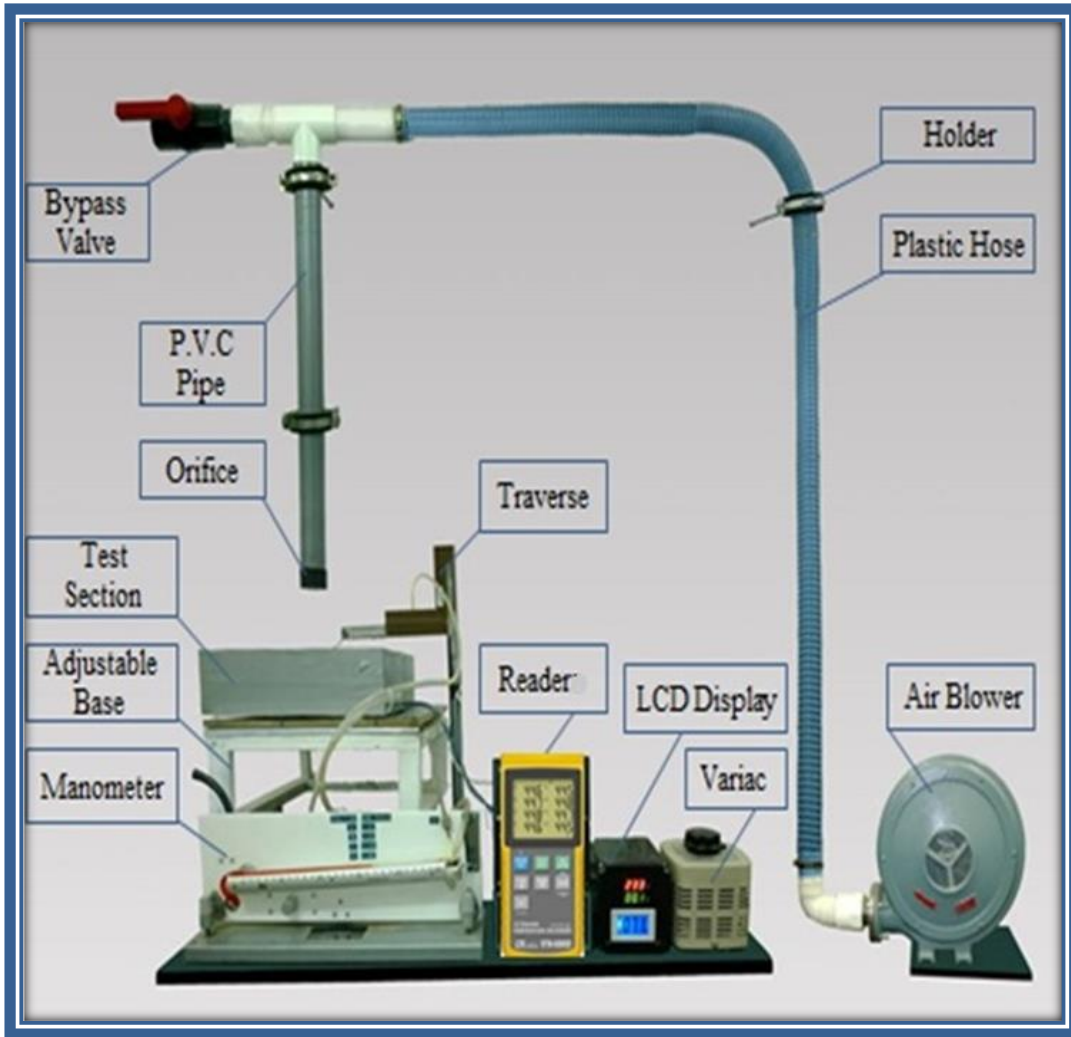


Figure 1. Experimental test rig

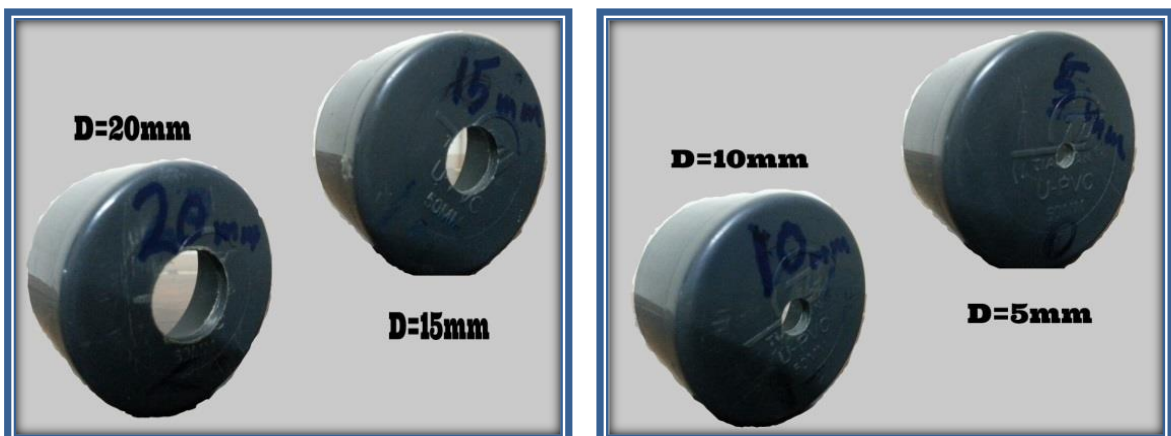


Figure 2. Photographs of orifice diameters

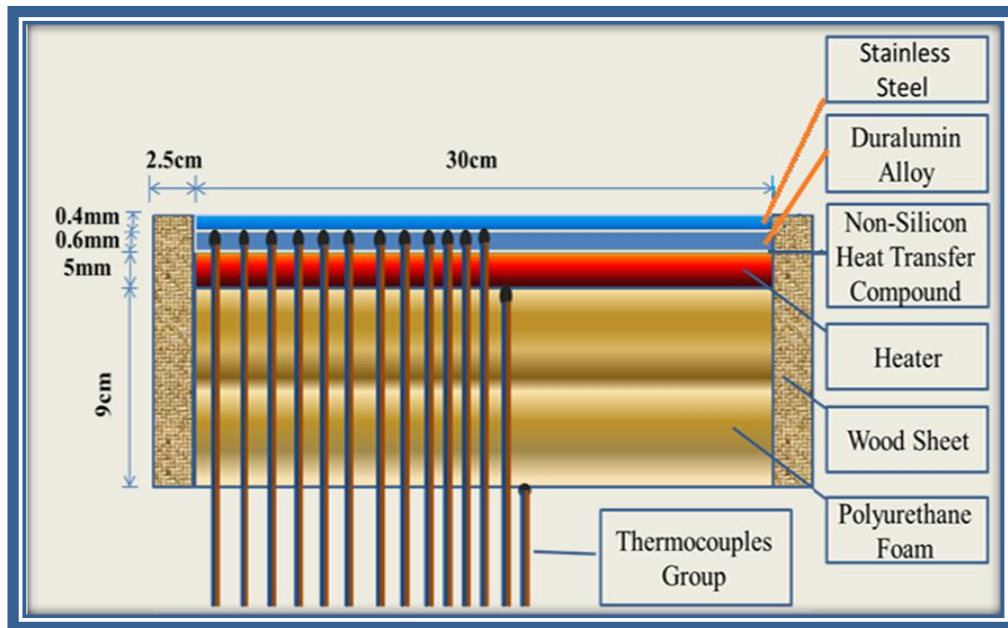


Figure 3. Schematic diagram of test section

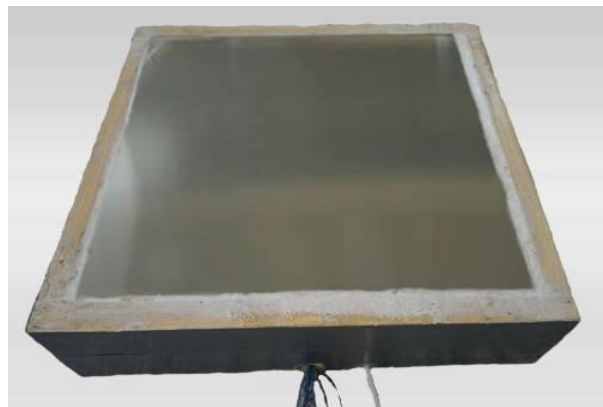


Figure 4. Photographs of a target plate fitted at test section

## 2.1 Measuring devices

**Air velocity:** using multi range manometer in range (0-250 mmH<sub>2</sub>O), it's have an air bubble type to ensure horizontal level during measurements. A total tube used to measure air velocity distribution at orifice exit and within wall jet region.

**Voltage and Current:** using a digital dual display LCD panel meter in range AC 80-300 V, AC 0-50 A with accuracy of  $\pm 1\%FS \pm 1$  digit.

**Temperature:** 12-channels model (BTM-4208SD) with SD card to save data along time with range 1 to 3600 seconds. Measuring range (-100 to 1300 °C) for type-K. Measuring temperature every 10 sec. from starting cooling till reach the target plate steady state condition, taken about 2000 second. Then, transferred data into lap-top by using 1G-SD.

### 3. Mathematical Formulation

The base plate under jet impingement can be modeled as semi- infinite solid having a boundary of surface convection. Consider that, heat transfer happened on  $x=0$  only by convection and negligible heat transfer by conduction and radiation. See Fig.5 .

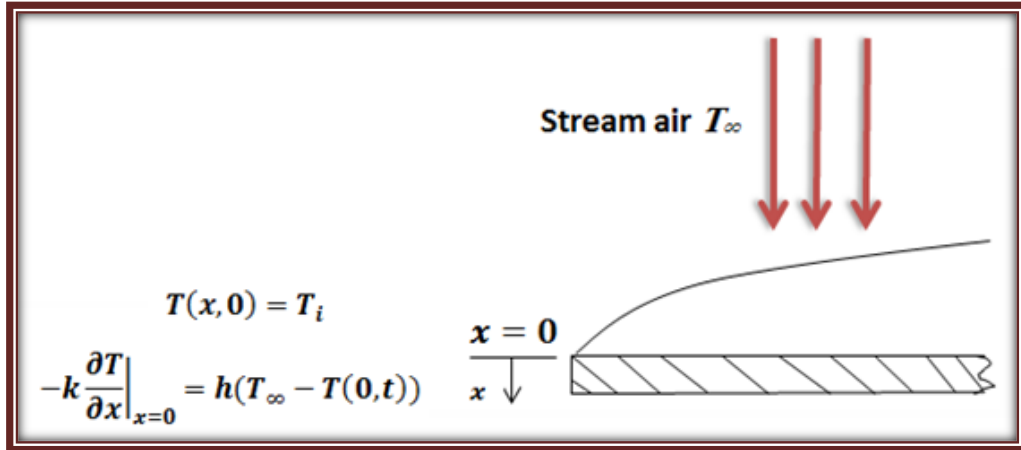


Figure 5. Schematic of flow over a flat plate

The temperature distribution on the target plate measured experimentally is used in (1) below:

$$\frac{T_s - T_i}{T_\infty - T_i} = 1 - \exp\left[-\frac{h^2 \alpha t}{k^2}\right] \operatorname{erfc}\left[\frac{h\sqrt{\alpha t}}{k}\right] \tag{1}$$

Therefore, the heat transfer coefficient ( $h$ ) can be determined by using try and error method. The above equation used to calculate heat transfer coefficient for transient period. These heat transfer coefficients represent local heat transfer coefficients which varies with position and time during the transient period till reaching the steady state condition. Table (1) represent the properties used in (1).

Table 1. Properties of air and stainless steel plate.

Properties	Value
$\rho_{air}$	$1.16 \text{ kg} / \text{m}^3$
$\mu_{air}$	$1.9 * 10^{-5} \text{ kg} / \text{m.s}$
$K_{air}$	$0.027 \text{ W} / \text{m.}^\circ\text{C}$
$\alpha_s$	$3.95 * 10^{-6} \text{ m}^2 / \text{s}$
$K_s$	$14.9 \text{ W} / \text{m.}^\circ\text{C}$

To calculate heat transfer coefficient at steady state by using the equations:

$$Q_{conv.} = Q_{input} - Q_{rad.} - Q_{cond.}$$

$$Q_{conv.} = hA_s(T_s - T_f)$$

$$q''_{conv.} = \frac{Q_{conv.}}{A_s} \longrightarrow h = \frac{q''}{T_s - T_f} \quad (2)$$

The velocity of jet can be calculated by using equation (3) for flow at jet exit.

$$U_j = \sqrt{2g\Delta h_w \frac{\rho_w}{\rho_{air}}} \quad (3)$$

The local Nusselt number as defined by equation (4) at any radial location (r).

$$Nu = \frac{hD}{K_{air}} \quad (4)$$

To calculate the average heat transfer coefficient and average Nusselt number following equations are used:

$$h_{avg} = \frac{1}{L} \int_0^L h_x dx \quad (5) \quad , \quad Nu_{avg} = \frac{1}{L} \int_0^L Nu_x dx \quad (6)$$

These values represent average values for the whole plate during each test in steady state condition.

Test procedure is carried out as follows in each test:

- 1- Turn on the air blower.
- 2- The dry air forced from blower is supplied through air supply valve was adjusted to allow a level of flow rate of air maintained in a certain fixed value.
- 3- Choosing orifice diameter D, four diameters are used in this work (D=5, 10, 15 and 20mm).
- 4- Jet velocity is determined for each orifice diameter tested, where there is four velocities for reach diameter with range from (18 to 40m/s).
- 5- Test section is placed at orifice to target plate (H/D) with correspond the location center of the target plate to the orifice center. For each jet velocity there is four distances with range (H/D=2, 4, 6 and 8).
- 6- Then turn on the heater wire and supply electrical power to the plate to heat it. The value of input power chosen for heating the target plate to a uniform

temperature rise in the range of 10-15 °C more than ambient temperature. Then exposing the plate to flow rate of the air for cooling the target plate.

- 7- Temperatures of target plate from starting cooling process at time (0 second) are recorded until steady state after (2000 second) are reached, so that temperatures have constant value without change. Temperature of the target plate are recorded at every (10 seconds).
- 8- 5-7 steps are repeated with varying H/D (2, 4, 6 and 8) values at the same orifice diameter and same jet velocity.
- 9- Steps from 4-7 are repeated with varying jet velocity at same orifice diameter with varying H/D.
- 10- Steps 3-7 are then repeated with varying orifice diameter D.
- 11- The recorded temperatures are taken to the lap-top and heat transfer coefficients and Nusselt numbers are calculated by using Microsoft Excel 2010 with applying equation (1) that solved by try and error method.

#### 4. Results and Discussions

An axisymmetric jet discharging from an orifice impinging normally onto a solid plate heated by a uniform heat flux was investigated. (64) test cases are performed for this investigation covering different parameters of orifice diameters D, jet velocities  $U_j$ , orifice to plate distance ratio (H/D). The results are based on calculated local and average heat transfer coefficient and Nusselt number for transient and steady state. Also, results show the behavior of transient state of different variables chosen for two periods of time and Nusselt number variation with distance from plate center and with different orifice to plate distance ratio using variable jet velocities.

Fig. (6) shows the Nusselt number distribution with total time in transient state given by parameter " $\tau_o$ " in range of ( $\tau_o = 0-1$ ) and with distance ratio from plate center ( $r/r_o$ ) for  $D=20\text{mm}$  and  $U_j=35.02\text{m/s}$  and  $H/D=4$ . The Nusselt number decreases monotonically from stagnation point outward to plate edge. This isn't surprising since fluid is being convected away from the stagnation region rapidly and loses its turbulence kinetic energy.

Fig. (7) shows the results of Nusselt number at steady state for  $D=20\text{mm}$  and  $U_j=35.02\text{m/s}$  and  $H/D=6$ . The maximum value of Nusselt number is found at stagnation point and is decreased with radial distance from plate center due to convected fluid away from stagnation region rapidly and loss its turbulence kinetic energy. At the stagnation point the boundary layer thickness is very small, so the heat transfer coefficient becomes larger at this point. The boundary layer thickness is increased away from plate center lead to decrease heat transfer coefficient.

The optimum orifice to target plate distance ratio is chosen corresponding to overall heat transfer coefficient for each orifice diameters with represented in Fig. (8,9). Figures show that optimum value of orifice to plate distance ratio H/D is to be 6 for  $D=20$  and  $15\text{mm}$  and it is 4 for  $D=10$  and  $5\text{mm}$ .

Results in Fig. (10,11) are declares the average heat transfer coefficient variation with distance from plate center from stagnation point towards target edge, with heat



transfer coefficients value being the higher for the period of ( $\tau_o = 0 - 0.1$ ) respective to the second mentioned period ( $\tau_o = 0.45 - 0.5$ ). This behavior is due to the fact that, the transient period elapsed with the hydrodynamic boundary layer and thermal boundary layer is being developed starting from stagnation point and reduced in the outward direction in the same way as in the case of steady state condition. The boundary layer thickness increases away from stagnation point. This is because of the reduction in wall jet momentum described by ordinary boundary layer behaviour and development of shear stresses with the plate surface in the outward direction. On the other hand, in the case of transient period the thermal boundary layer is being developed without thickness at start of cooling, so the heat transfer coefficient is with its highest value then reduces when the thermal boundary layer is developed.

In fig. (12,13), two cooling periods are taken at cooling period ( $\tau_o = 0 - 0.1$ ) and ( $\tau_o = 0.45 - 0.5$ ) with ( $H/D=6$ ). It is noticeable that larger orifice diameter gives higher heat transfer coefficients. At interval time ( $\tau_o = 0 - 0.1$ ) the average heat transfer coefficient is substantially decreased in radial distance. After this time interval ( $\tau_o = 0.45 - 0.5$ ) the average heat transfer coefficient is slightly decreased from the previous interval for all cases. The distributions of average heat transfer coefficient for various radial directions are much more uniform than the previous time interval. The heat transfer converges to steady state after about 2000 sec. As mentioned before, the maximum obtained value of Nusselt number is found at stagnation point and is decreased with radial distance from the plate center. As the radial distance increases, the velocity decreases because the cross-sectional area of the flow in the wall jet region increases, and consequently the Nu and heat transfer coefficient decreases as well. Also it can be noticed that small orifice sizes gives lower heat transfer coefficients, so Nusselt number decreases with decreasing orifice sizes attributed to small momentum of jets of small orifice size, with shorter potential flow core.

In order to understand in great details the relations of the stagnation heat transfer coefficient and overall heat transfer coefficient for transient time since 2000 second and for plate radial distance from center. This is shown in Fig. (14,15). It is obvious that the stagnation heat transfer coefficient greater than the overall heat transfer coefficient at all cases. It can be noticed that bigger diameter stagnation values are relatively closer to the overall transfer values compared to the smaller diameter due to the fact that small diameter heat transfer coefficient distribution decays in a high rate due to lower momentum and smaller area coverage. Also Figures show that, high air jet velocity gives higher jet momentum which means higher penetration rate. Low air jet velocities are gives smaller effect on heat transfer enhancement because of low jet momentum and due to lower Reynolds number.

Average heat transfer in transient period to steady heat transfer coefficient ratio has seen in Fig. (16,17). Fig. (16) show that the ratio is high at the start of cooling period with the ratio being in the range of 2-3 times then reduces reaching about unity for the record period of cooling. It can be seen that at interval time ( $\tau_o = 0 - 0.1$ ) with increasing radial distance from the stagnation point the heat transfer coefficient ratio decreases slightly and maximum ratio is at ( $H/D=4$ ). After this time interval ( $\tau_o = 0.45 - 0.5$ ) with increasing distance from the center heat transfer coefficient ratio continue to reduce from previous period and optimum ratio is at ( $H/D=4$ ).

Transient heat transfer coefficient to steady heat transfer coefficient has seen in Fig. (18,19), show how these various with the interval time ( $\tau_o = 0 - 1$ ) at radial plate distance. It is noted that as the beginning period the ratio heat transfer coefficient on impingement surface is increased until reach a peak at interval time ( $\tau_o = 0.015$  for

both  $H/D=2$  and  $4$ ,  $\tau_o=0.025$  for  $H/D=6$  and  $\tau_o=0.02$  for  $H/D=8$ , the maximum heat transfer fluctuation now occurs at the center of the jet and then decreases radially. The heat transfer converges to steady state and decreases which affects the turbulence characteristics of the flow at the time beginning.

## 5. Development of Correlations

Nusselt number correlations have been developed with the help of relevant dimensionless groups involving parameters like orifice-to-target plate spacing  $H/D$ , Reynold number, Prandtl number, distance ratio from the plate center  $r/r_o$  and total time to steady time ratio  $\tau_o$ . In analyzing the experimental data for the effect of the individual dimensionless group, the values of constant ( $K$ ) and the exponent ( $a-f$ ) have been obtained by using LAB Fit curve fitting software-version 7.2. The LAB Fit is software for Windows developed aiming the treatment and the analysis of experimental data and determines propagated error (error propagation up to eight independent variables).

Parameters:  $Nu$ ,  $Re$ ,  $(Pr)^{0.33}$ ,  $\frac{H}{D}$ ,  $\frac{t}{t_\infty}$  have been considered as the input parameters from experimental data.  $K$  (overall coefficient), and ( $a-f$ ) (individual exponents of these parameters) have been considered as the output for the LAB Fit software training of the data.

### 5.1 Transient Correlations

The developed correlation of Dimensional Analysis (DA) approach for stagnation Nusselt number in transient state since 2000 second is as follows:

$$Nu_{Stag.} = K Re^a (Pr)^{0.33} \left(\frac{H}{D}\right)^b \left(\frac{t}{t_\infty}\right)^c \quad (7)$$

$$Nu_{Stag.} = 0.0749 Re^{0.781} (Pr)^{0.33} \left(\frac{H}{D}\right)^{-0.0522} \left(\frac{t}{t_\infty}\right)^{-0.0918} \quad (8)$$

Developed correlation of Dimensional Analysis (DA) approach for Nusselt number along plate distance from the plate center for transient state since 2000 second is as follows:

$$Nu_{r/r_o} = Nu_{Stag.} \left(\frac{r}{r_o}\right)^d \quad (9)$$

Where  $Nu_{Stag.}$  obtained from correlation (5.2), value of the exponent ( $d$ ) has been obtained by using LAB Fit software since 2000 second.

$$Nu_{r/ro} = 0.0749 \text{ Re}^{0.781} (\text{Pr})^{0.33} \left(\frac{H}{D}\right)^{-0.0522} \left(\frac{t}{t_\infty}\right)^{-0.0918} \left(\frac{r}{r_o}\right)^{0.1941} \quad (10)$$

The latest developed correlation of Dimensional Analysis (DA) approach for average Nusselt number along plate distance from the plate center for transient state since 2000 second is as follows:

$$Nu_{Av.} = K \text{ Re}^e (\text{Pr})^{0.33} \left(\frac{H}{D}\right)^f \quad (11)$$

$$Nu_{Av.} = 0.1550 \text{ Re}^{0.727} (\text{Pr})^{0.33} \left(\frac{H}{D}\right)^{-0.0445} \quad (12)$$

## 5.2 Steady state Correlations

The developed correlation of Dimensional Analysis (DA) approach for stagnation Nusselt number in steady state after 2000 second is as follows:

$$Nu_{Stag.} = K \text{ Re}^a (\text{Pr})^{0.33} \left(\frac{H}{D}\right)^b \quad (13)$$

$$Nu_{Stag.} = 0.3078 \text{ Re}^{0.608} (\text{Pr})^{0.33} \left(\frac{H}{D}\right)^{-0.092} \quad (14)$$

The latest developed correlation of Dimensional Analysis (DA) approach for average Nusselt number along plate distance from the plate center for steady state after 2000 second is as follows:

$$Nu_{Av.} = K \text{ Re}^c (\text{Pr})^{0.33} \left(\frac{H}{D}\right)^d \quad (15)$$

$$Nu_{Av.} = 0.453 \text{ Re}^{0.509} (\text{Pr})^{0.33} \left(\frac{H}{D}\right)^{-0.0463} \quad (16)$$

The dimensionless presentation of heat transfer measurements according to the correlation is plotted on logarithmic scale for transient and steady state as shown in Fig. (20). A comparison between the stagnation Nusselt number correlated in present work with the same model of Anwarullah [7] is presented in Fig. (21).

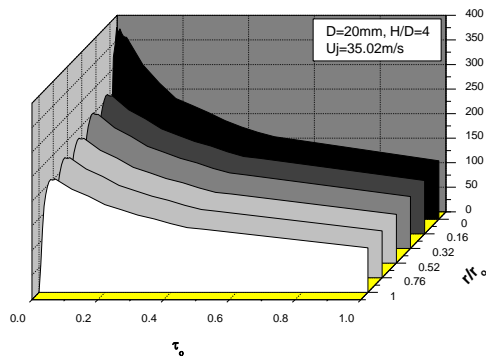


Figure 6. 3-D curve of local Nusselt number, D=20mm, H/D=4, Uj=35.02m/s

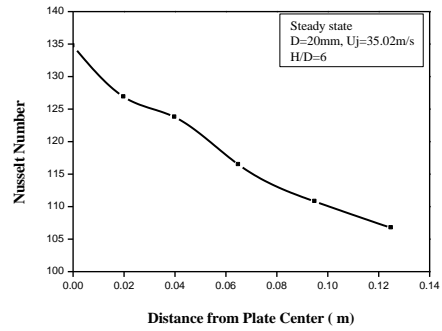
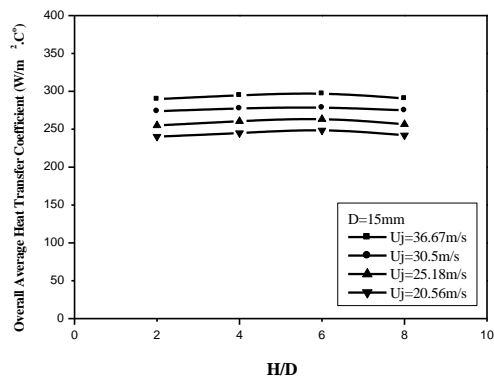
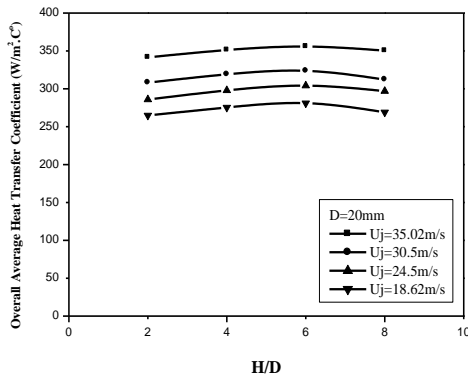
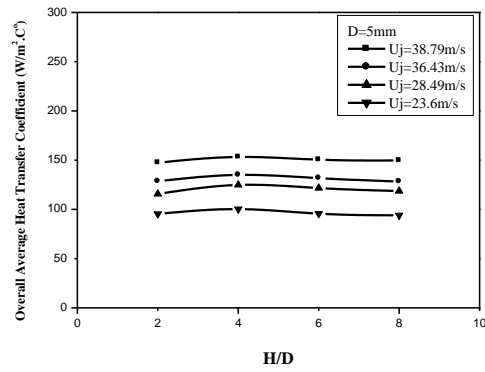
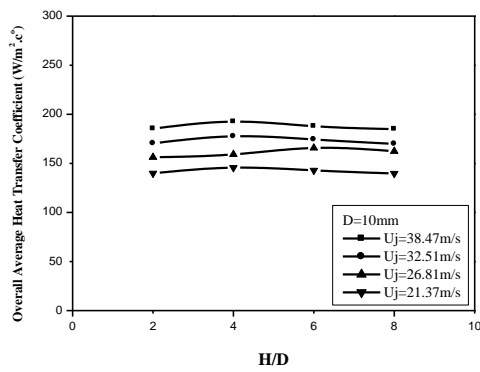


Figure 7. Local Nusselt number at  $\tau_o = 1$ , for D=20mm, H/D=6, Uj=35.02m/s



Figures 8. Variation of overall average heat transfer coefficient for D=20, 15mm



Figures 9. Variation of overall average heat transfer coefficient for D=10, 5mm

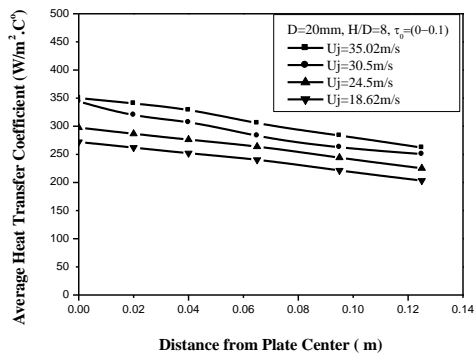


Figure 10. Variation of average heat transfer coefficient at  $\tau_o = 0 \rightarrow 0.1$

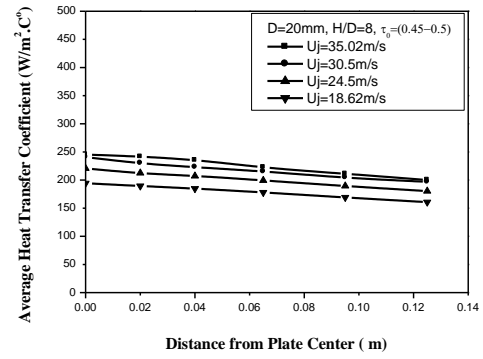


Figure 11. Variation of average heat transfer coefficient at  $\tau_o = 0.45 \rightarrow 0.5$

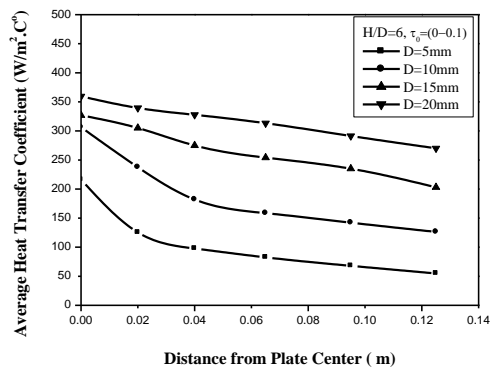


Figure (12): Variation of average heat transfer coefficient at  $\tau_o = 0 \rightarrow 0.1$

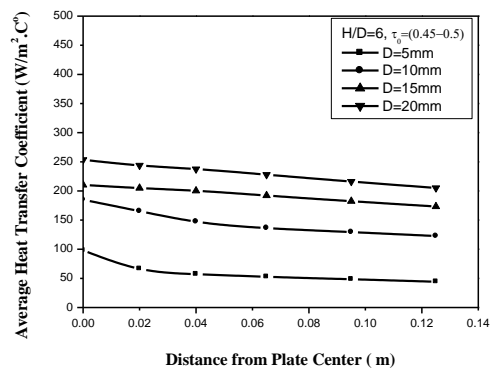
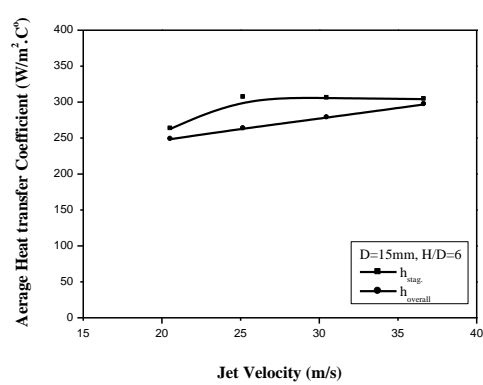
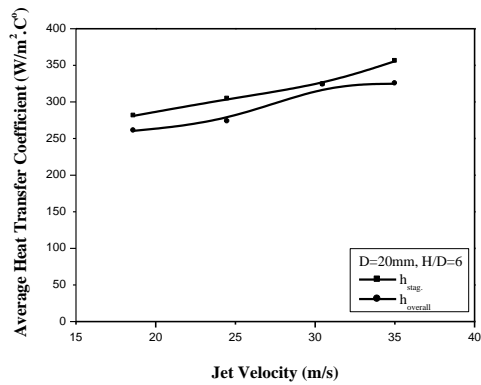
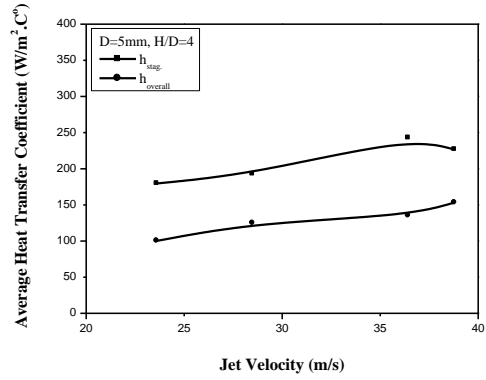
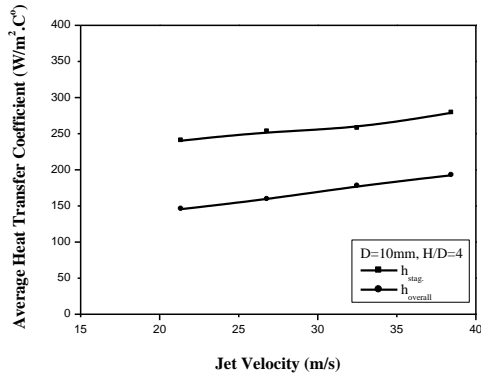


Figure (13): Variation of average heat transfer coefficient at  $\tau_o = 0 \rightarrow 0.1$



Figures 14. Variation of average heat transfer coefficient with jet velocity for D=20,15mm, H/D=6



Figures 15. Variation of average heat transfer coefficient with jet velocity for D=10,5mm, H/D=4

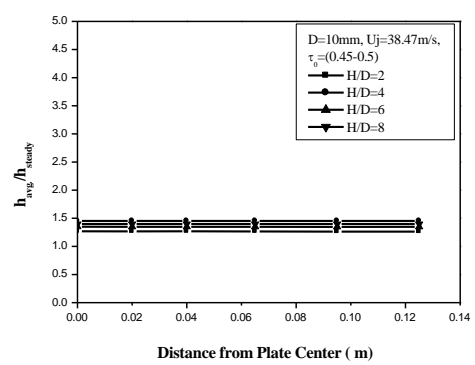
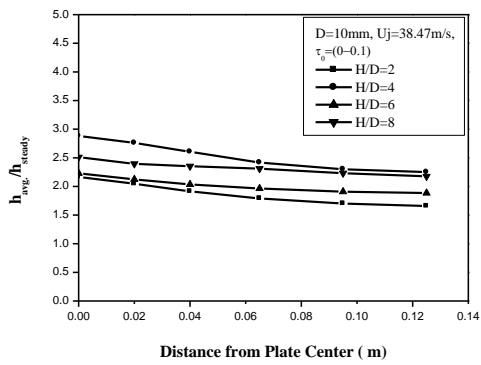
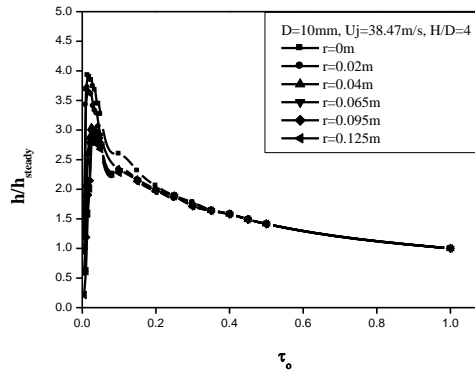
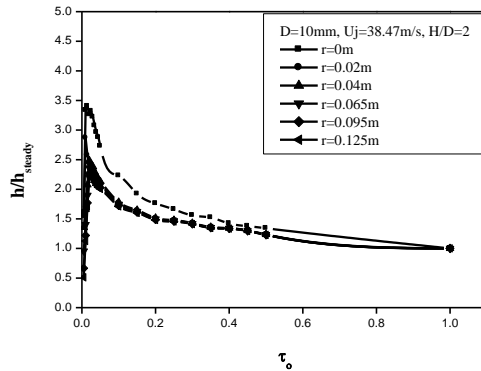
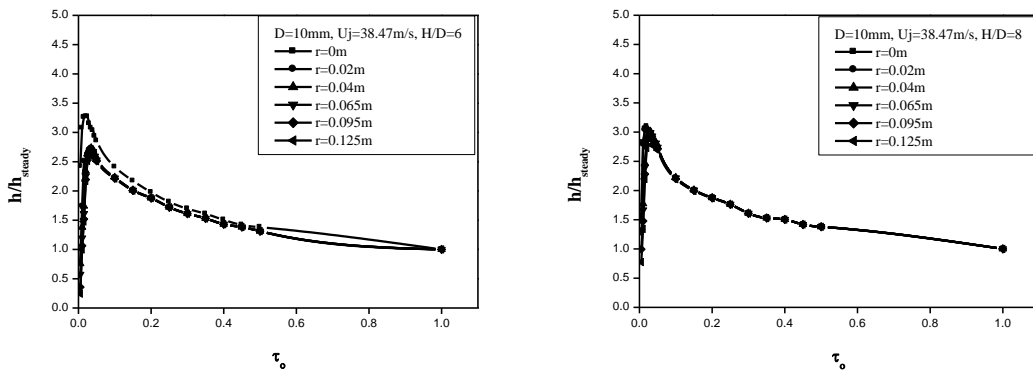


Figure 16. Ratio between average and steady heat transfer coefficient at  $\tau_o = 0 \rightarrow 0.1$ , for D=10mm

Figure 17. Ratio between average and steady heat transfer coefficient at  $\tau_o = 0.45 \rightarrow 0.5$ , for D=10mm



Figures 18. Ratio between local and steady heat transfer coefficient, H/D=2,4



Figures 19. Ratio between local and steady heat transfer coefficient, H/D=6,8

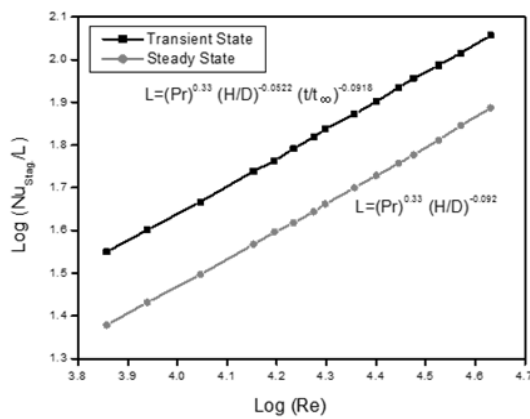


Figure 20. Dimensionless presentation of heat transfer measurements in transient and steady state

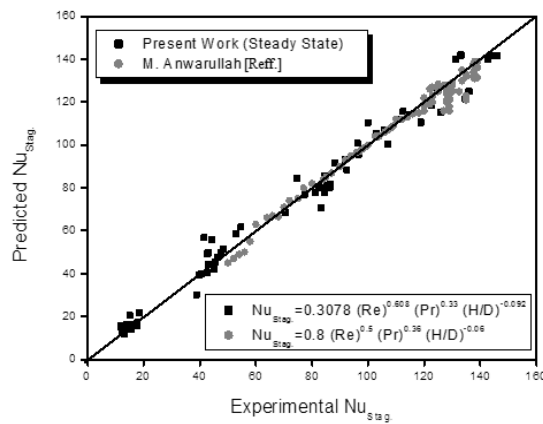


Figure 21. A comparison of present work results with [7] for predicted and experimental stagnation Nusselt number

## 6. Conclusions

The present work has included the following :

- 1- Record the temperature distribution of the target plate during transition period till reach the plate to steady state for different orifice diameters (D =5,10,15 and 20mm), jet velocities range from (Uj=18 – 40m/s) and orifice to plate distances (H/D=2,4,6 and 8).
- 2- It's found the plate taken about 2000 second to be steady state, during this period recorded temperatures every 10 second on six positions on the target plate and apply the transient of semi-infinite solid equation that solved by using try and error method.
- 3- Calculate the heat transfer coefficient and Nusselt number for transient and steady state with position on the target plate and compares between them.
- 4- Form 64 cases, it's found the heat transfer coefficient increases with jet velocity and orifice diameters increasing for both transient and steady state.
- 5- The optimum value of H/D is 6 at (D=20 and 15mm) and its 4 at (D=10 and 5mm) at transient state, while its found the optimum value of H/D at steady state is 6 for

maximum velocity and  $H/D=4$  for minimum velocity for ( $D=20\text{mm}$ ),  $H/D=2$  for both maximum and minimum velocity for ( $D=15\text{mm}$ ),  $H/D=6$  for maximum velocity and  $H/D=2$  for minimum velocity for ( $D=10\text{mm}$ ) and  $H/D=8$  for both maximum and minimum velocity for ( $D=5\text{mm}$ ).

- 6- Determine correlations at transient state comprised Nusselt number at stagnation point as function of time, Nusselt number at any position on the target plate and overall average Nusselt number for all target plate.
- 7- Correlations have been developed with the help of relevant dimensionless groups, involving interacting parameters by using dimensional analysis (DA).

## 7. Nomenclature

Character	Latin Characters Description	Units
$A_s$	Surface cross sectional area of the plate	$\text{m}^2$
$D$	Orifice diameter	$\text{m}$
$d_x$	Infinitesimal length of one node of the plate	$\text{m}$
$H/D$	Orifice diameter to target plate distance ratio	–
$h$	Heat transfer coefficient	$\text{W}/\text{m}^2.\text{C}^\circ$
$h_{\text{avg}}$	Average heat transfer coefficient	$\text{W}/\text{m}^2.\text{C}^\circ$
$h_{\text{steady}}$	Heat transfer coefficient at steady state	$\text{W}/\text{m}^2.\text{C}^\circ$
$h/h_{\text{steady}}$	Heat transfer coefficient at transient state to steady state ratio	–
$K_{\text{air}}$	Thermal conductivity of exit air from jet	$\text{W}/\text{m}.\text{C}^\circ$
$\text{Nu}_{\text{stag.}}$	Stagnation Nusselt number	–
$\text{Pr}$	Prandtl number	–
$Q_{\text{input}}$	Total input power	$\text{W}$
$Q_{\text{rad.}}$	Heat losses by radiation	$\text{W}$
$Q_{\text{cond.}}$	Heat losses by conduction	$\text{W}$
$Q_{\text{conv.}}$	Convection heat transfer	$\text{W}$
$q_{\text{conv.}}''$	Heat flux	$\text{W}/\text{m}^2$
$r$	Radial distance from the plate center	$\text{m}$
$r_o$	Length of larger area on the plate	$\text{m}$
$t$	Time	Second
$T_f$	Film temperature	$\text{C}^\circ$
$T_i$	Initial temperature	$\text{C}^\circ$
$T_s$	Surface temperature	$\text{C}^\circ$
$T_j$	Stream jet temperature	$\text{C}^\circ$
$T_\infty$	Ambient temperature	$\text{C}^\circ$
$\tau_o$	Total time to steady time ratio	
$U_j$	Jet velocity	$\text{m}/\text{s}$
$\Delta h_w$	Head of water for manometer reading	$\text{M}$



Character	Greek Symbols Description	Units
$\pi$	Relative constant	-
$\alpha_s$	Thermal diffusivity of stainless steel plate	$\text{m}^2/\text{s}$
$\rho_{air}$	Density of air exit from jet	$\text{Kg}/\text{m}^3$
$\rho_w$	Water density	$\text{Kg}/\text{m}^3$
$\mu_{air}$	Dynamic viscosity of air exit from jet	$\text{N.s}/\text{m}^2$

#### Subscripts

avg.	Average
DA	Dimensionless Analysis
sec.	Second
stag.	Stagnation

### Acknowledgement

Allah, the creator is thanked for everything before all, I would like to express my deepest thanks and sincere gratitude to my supervisors Prof. Dr. Adnan A. Abdel Rasolo and Dr. Dhamia'a Saad Khudor for their assistance, guidance, encouragement and endless help throughout the steps of this work.

### 8. References

1. Raghav, G.H. (2014). *"Numerical Analysis of Hydraulic Jump by an Impinging Jet"*. M.Sc. thesis, Department of Mechanical Engineering; National Institute of Technology, Rourkela.
2. Hyung, H.C. and Kyung, M.K. (2011). *"Applications of Impingement Jet Cooling Systems"*. Cooling Systems: Energy, Engineering and Applications. Nova Science Publishers Inc., Yonsei University, Chapter 2.
3. Incropera, F.P. (2011). *"Fundamentals of Heat and Mass Transfer"*. 7<sup>th</sup> ed., John Wiley and Sons Series.
4. Islam, M. and Rezwan, A. (2011). *"Study of Transient Heat Transfer of a Solid with Protective Fabric under Hot Air Jet Impingement"*. Int. Conf. on Mechanical Engineering, PP.1-6.
5. Mark, M.D. (2011). *"Steady and Transient Heat Transfer for Jet Impingement on Patterned Surfaces"*. M.Sc. thesis, Department of Mechanical Engineering; University of South Florida.
6. Colin, G. and Tadhg, O. *"Jet Impingement Cooling"*. CTVR (Centre for Telecommunications Value-Chain-Driven Research), Department of Mechanical and Manufacturing Engineering, Trinity College, Dublin, PP.1-9.
7. Anwarullah, M. (2012). *Effect of Nozzle Spacing on Heat Transfer and Fluid Flow Characteristics of an Impinging Circular Jet in Cooling of Electronic Components*.

- International Journal of Thermal and Environmental Engineering, Vol. 4, No. 1, PP.7-12.
8. Nawaf, H.S. (2009). *"Effect of Oscillating Jet Velocity on the Jet Impingement Cooling of an Isothermal Surface"*. Department of Mechanical Engineering, Manufacturing and Materials Engineering, University of Nottingham Malaysia Campus, 1, PP.133-139.
  9. Vadiraj, K. and S.V. (2008). *Experimental Study and Theoretical Analysis of Local Heat Transfer Distribution between Smooth Flat Surface and Impinging Air Jet from a Circular Straight Pipe Nozzle*. International Journal of Heat and Mass Transfer, Vol.51, pp. 4480–4495.
  10. Chung, Y.M. and Luo, K.H. (2002). *Numerical Study of Momentum and Heat Transfer in Unsteady Impinging Jets*. International Journal of Heat and Fluid flow 23, PP.592-600.
  11. Chitranjan, A. (2012). *Jet Impingement Cooling of Hot Horizontal Surface Through Sharp Edge Nozzle*. International Journal of Applied Engineering and Technology, Vol. 2 (3), PP.14-17.
  12. Hee, J.P. *"Heat Transfer from a Pulsed Laminar Impinging Jet"*. Department of Mechanical Engineering, National University of Singapore, pp.1-10.
  13. Alan, M., Tim, P. (2008). *"Heat Transfer Measurements of an Impinging Synthetic Air Jet with Constant Stroke Length"*. 5<sup>th</sup> European Thermal Science Conference, The Netherlands, PP.1-8.
  14. Herbert, M.H. and Matthias, K. (2007). *Measurements on Steady State Heat Transfer and Flow Structure and New Correlations for Heat and Mass Transfer in Submerged Impinging Jets*. International Journal of Heat and Mass Transfer, Vol.50, pp.3957–3965.
  15. Holman, J.P. (2002). *"Heat Transfer in SI Units"*. 9<sup>th</sup> ed., McGraw-Hill.
  16. Humam, K.J. (2013). *"Study the Effect of Holed Arc Trench of Compound Orientation Angle on Surrounding Flow Field and Film Cooling Performance"*. M.Sc. thesis, Department of Mechanical Engineering; University of Technology, Iraq.